SURFACE PATTERNING IN Ge-Se AMORPHOUS LAYERS

I. Csarnovics*[1], M. Veres[2], P. Nemec[3], M. R. Latif[4], P. Hawlova[3], S. Molnar[1], S. Kokenyesi[5]

[1] Department of Experimental Physics, University of Debrecen, Debrecen, Hungary

[2] Institute of Solid State Physics and Optics, Wigner RCP, HAS, Budapest, Hungary

[3] Department of Graphic Arts and Photophysics, Faculty of Chemical Technology, University of Pardubice, Pardubice, Czech Republic

[4]Department of Electrical and Computer Engineering, Boise State University, Boise, ID, USA

[5] Department of Electrical Engineering, University of Debrecen, Debrecen, Hungary

Abstract

Compositional and fabrication method dependences of laser-induced geometrical surface relief formation in Ge-Se amorphous layers were investigated with the aim to determine the possible role of initial conditions in the mechanism and efficiency of optical recording. The results show that pulsed laser deposition has some advantages in composition preservation and surface relief formation in comparison with thermal evaporation for producing layers with high sensitivity and efficiency of surface relief grating formation, especially in layers with $Ge_{24}Se_{76}$ composition. It was shown that modulation depth of the created surface structures increases with increasing Se content in Ge-Se amorphous chalcogenide layers. Thermal annealing has essential influence on the recording parameters, enabling additional insight into the possible mechanisms of light induced surface patterning in this type of light-sensitive amorphous chalcogenides. Raman spectroscopy was used to identify local structure of produced surface patterns.

Keywords: amorphous chalcogenides, Ge-Se system, thin films, light induced surface patterning, Raman spectroscopy, atomic force microscopy.

*corresponding author: Istvan Csarnovcs, e-mail: csarnovics.istvan@science.unideb.hu, tel.: +36-70-331-4744, address: 18/a Bem sq, Debrecen, Hungary, 4026.

1. Introduction

Among the many practically important properties of chalcogenide glasses, the photo-induced effects which can be initiated with visible light impress with their variety. This class of material exhibits well known photo-induced structural transformation effects of the amorphous phase and related changes of optical parameters (absorption coefficient, refractive index) under the influence of photons with energy close to the band gap (E_g) energy [1-3]. Some peculiar effects like photo-plasticity or photo-fluidity [4,5], photo-stimulated expansion or contraction and mass-transport [3,6,7] were also observed and can be used for optical amplitude-phase relief recording. For the As-Se system for example, the character and magnitude of such effects are known as essentially dependent on the composition [8]. The characteristics of recording are affected also by the technology of thin film fabrication [9-11] that can be related to the structural state of the amorphous film obtained by different films' deposition methods and treatment processes. The latter can be the reason for different results regarding the magnitude, type (darkening vs. bleaching), stability and repeatability of the optical recording processes in a number of compositions, especially in these with higher softening temperatures (150-400 ^{0}C) like the Ge-Se system, which was not well investigated yet.

During the last decade, a number of papers were devoted to the investigations of surface deformations and direct recording of surface geometrical reliefs, mostly holographic gratings, in different chalcogenide layers from As-S(Se) systems [8,12,13]. It has been established, for example, that the evolution of surface relief in $As_{20}Se_{80}$ contains two distinct parts. First part is fast (few seconds), with a comparatively small increase of the volume, which is connected with bond breaking, rearrangement and the free volume change (up to 1-2 %). The second part, which is much slower, results in more significant thickness change (up to 10-20 % or even complete transport of the material between illuminated and non-illuminated parts), and it is connected with the effect of lateral mass transport [12,13].

Less data are available for the Ge-Se amorphous chalcogenide layers, which are light sensitive in the green-red spectral region [14,15]. Photo-induced optical effects, volume changes and the possibility of holographic recording were also investigated earlier [16,17]. However, the mechanism of the photo-induced volume changes in Ge-Se system is not completely clear yet. Among others the white spots in this field can be explained by the absence of correlations of the film fabrication technology and sample treatment vs. photo-induced effects in Ge-S(Se) thin films.

Chalcogenide thin films can be obtained by different techniques such as radio-frequency sputtering or thermal vacuum evaporation (TE) [18,19]. The latter was successfully used for the fabrication of not only single, but also multilayered structures from the As-S(Se) system [20]. Pulsed laser deposition (PLD) was used earlier to create chalcogenide based single and multilayer nano-structures [21-23]. We already reported PLD as a thin film/multilayered structure fabrication technique viable for the Ge-based amorphous chalcogenides, because of the easy control of the process and often stoichiometric transfer of target material to the films [23-25]. In this work we used both TE and PLD methods for the preparation of thin layers based on Ge-Se amorphous chalcogenides.

The aim of this work is to investigate the compositional dependence of the light induced surface pattern formation, structural and volume changes in TE and PLD Ge-Se thin films. Besides, an attempt to explain the influence of the initial state (as-deposited or annealed) of the samples on the observed effects is presented. Finally, our attention was directed to find the best conditions (composition, recording parameters, and initial state of the samples) for holographic recording within studied materials. This could be eventually used for the creation of surface relief elements for different applications.

2. Experimental

Bulk chalcogenide glasses from Ge-Se system were synthesized in silica ampoules from high-purity (typically 99.999%) elements by melt-quenching method and used for the deposition of amorphous layers via the both above mentioned techniques. The TE method with a Cressington 308R thermal evaporation system at $1x10^{-6}$ mbar pressure, using a semi Knudsen cell crucible charged with the source material was used. Evaporation of charges with $Ge_{20}Se_{80}$ and $Ge_{27}Se_{73}$ composition resulted in formation of films with composition $Ge_{28}Se_{72}$ and $Ge_{33}Se_{67}$. On the other hand, employing PLD with $Ge_{20}Se_{80}$ and $Ge_{27}Se_{73}$ glassy targets, films with $Ge_{24}Se_{76}$ and $Ge_{30}Se_{70}$ composition were prepared. PLD setup consisted of a KrF excimer laser (248 nm, 300±3 mJ per pulse, 30 ns pulse duration, 20 Hz repetition rate) and vacuum chamber (background pressure $<4x10^{-6}$ mbar). The substrates used for PLD (chemically cleaned microscope glass slides and Si wafers) were positioned parallel to the target surface at a target to substrate distance of 5 cm. The laser energy fluency on the target was set to ~2.6 J/cm^2.

The composition of the samples was determined by Energy Dispersive X-Ray Spectroscopy (EDS) using Hitachi S-4300 Scanning Electron Microscope (SEM) system. It was established, that the composition changed differently depending on the Ge content of the precursor material and the preparation method, better preservation was achieved by PLD method. The thickness *d* of the samples was controlled by *in situ* and *ex situ* (by using variable angle spectroscopic ellipsometry) for the TE and PLD, respectively. Resulting thicknesses were about 1000 nm for the TE and 500 nm for the PLD films.

The optical transmission spectra of the created samples were measured with Shimadzu UV-3600 spectrophotometer. The surface patterns on the created samples were recorded at atmospheric pressure with laser setup operating in the region of short-wavelength absorption edge of the investigated materials. Holographic gratings with 6 μm period were recorded by two p-polarized and one additional s-polarized laser beam (Figure 1), as this configuration has the most significant effect in amorphous chalcogenides [26]. Surface patterns were created on as-deposited and annealed samples by a laser setup with an output power of 34 mW/cm^2 operating at 533 nm, since the samples are most sensitive in the green part of the spectra. The surface gratings were formed through 4 hour recording cycles. The surface of holographic gratings was investigated by atomic force microscope (AFM Veeco diCaliber) which also gave information about the average height of the created structures. The samples were investigated in tapping mode with TESP-MT probes. The gratings were investigated in 10 different areas in order to collect statistical data about their properties. The error of the measurements was about 2-3 %.

The annealing was performed below corresponding Ge-Se glass transition temperature T_g (at 170 ^{0}C for films with composition $Ge_{24}Se_{76}$ (PLD) and $Ge_{28}Se_{72}$ (TE) and at 270 ^{0}C for $Ge_{30}Se_{70}$ (PLD) and $Ge_{33}Se_{67}$ (TE)) for 2 hours in Ar atmosphere. Ambios XP-1 profilometer was used to determine the sample thickness before and after heat treatment. The subsequent EDS measurement showed that the composition of the samples has not changed for all samples, while the thickness of the samples decreased about 20 nm.

The structural changes due to surface patterning (on the hillocks and valleys of the created structures) and annealing were revealed by Raman spectroscopy using a Renishaw 1000B micro-Raman spectrometer with a 785 nm diode laser as excitation source. The Raman spectra were measured in the 150-400 cm^{-1} region with spectral resolution of 1 cm^{-1}. The beam diameter of the exciting light was approximately 1 μm, while the intensity in this experiment was limited (originally it was 5 mW/cm^2, but we used 0.5 mW/cm^2) in order to avoid

damage and additional photo-structural transformation of the samples. The spectra were baseline-corrected, normalized and the peaks were fitted with a set of Gaussians within the Microcal Origin software.

3. Results and discussion

1. Optical transmission and recording of holographic grating

Figure 2a represents the spectral dependence of the transmission for the studied as-deposited films. It can be seen that the position of the short-wavelength absorption edge and consequently the light sensitivity of the prepared samples to the 533 nm light used for the illumination depend on the Ge concentration and thin film deposition technique. The differences in the interference fringes ($Ge_{24}Se_{76}$ vs. $Ge_{28}Se_{72}$ and $Ge_{30}Se_{70}$ vs. $Ge_{33}Se_{67}$) are due to the different thicknesses of the samples. Annealing of the as-deposited samples below the glass transition temperature caused bleaching or increase in their transmission, so the optical absorption edge shifted to the shorter wavelength region in all samples (Figure 2b).

Holographic gratings were recorded in order to demonstrate the application feasibility of the photo-induced effects in Ge-Se films. Surface relief gratings were recorded on the as-deposited and annealed samples by two coherent p-polarized and one additional s-polarized laser beams, having equal intensity. As a result of this recording scheme a stable surface structure was formed. The main role of the additional (s-polarized) beam is to enhance the rate of mass transport, presumably through the extra dipolar effect, which increases the mass transport if the polarizations of the recording and additional beams are orthogonal [27]. Formation of a good quality surface pattern was achieved at average exposure of about 690 J/cm^2. This value was established as optimum for this type of chalcogenide layers. The created surface patterns were found to be stable for long periods of time and do not show any tendency for relaxation. Typical AFM images of the recorded holographic gratings are shown in Figure 3.

The modulation depth of the gratings on different samples varies in a wide range between 15-480 nm (Table 1). It can be seen that the increase of the Ge content in the films results in shallower holographic gratings. The highest surface patterns were observed for the $Ge_{24}Se_{76}$ and $Ge_{28}Se_{72}$ films. In detail, the modulation depth of the created holographic gratings reaches about 320 nm for annealed $Ge_{24}Se_{76}$ composition, i.e. about 64 % of initial film thickness. In addition, it was found that the modulation depth of the created surface relief was higher for the annealed samples at equal exposure conditions. At maximum, the depth increased from 240 to 480 nm, for the annealed $Ge_{28}Se_{72}$ sample. As it was mentioned in the Introduction part the photo-induced volume

changes in Ge-Se system were studied before [16, 17], however the compositional dependence of the process was not established yet and structures with such remarkable modulation depth were not obtained earlier.

From the above results it is clear that the hillock formation could not be caused by a simple photo-induced expansion of the film material, but rather by lateral mass transfer induced by light, which produces surface patterns and can be referred to as giant due to its prominence. The relief formation strongly depends on the composition and also on thermal prehistory of the samples (as-prepared or annealed) and, surprisingly, the modulation depth of the created holographic gratings is far more prominent in annealed films.

According to the results, the best conditions for the surface patterning in studied Ge_xSe_{100-x} thin films are near the x=24-28 composition. Therefore, further investigations were aimed at detailed characterization of these samples via Raman spectroscopy.

2. Raman spectroscopic investigations

The structure of the fabricated gratings was investigated via micro-Raman spectroscopy for both as-deposited and annealed samples in three regions: in the non-irradiated part, on the hillocks and in the valleys (Figure 4). For Ge_xSe_{1-x} bulk glasses four main Raman-active vibrational modes, which were also observed in our experiments, are known: a band peaking at 192-201 cm^{-1} (CS, corner-sharing $GeSe_4$ tetrahedra symmetric stretching vibration mode), an accompanying sideband near 210-218 cm^{-1} (ES, edge-sharing $GeSe_4$ tetrahedra mode), a broad band near 255-270 cm^{-1} (SE, Se-Se vibrations) and a band at 178 cm^{-1} observed in glasses/films with higher Ge content, corresponding to the formation of Ge-Ge bonds in ethane-like structural entities (ETH mode) [28-31]. These Raman bands show some dependence on the composition in our samples. From the measured Raman data, the individual bands' parameters were determined by fitting.

The following analysis focuses mainly on the Raman bands' area and to some extent on their widths. The first determines the changes of the concentration of the different building blocks in the structure, while peak width (and position) characterizes the bonds and their surrounding in different structural units [32]. In addition, since it is difficult to obtain comparable absolute bands' intensities, the bands' area ratios were used to characterize the structural changes in the films. Obviously, fitting gives also peak position data, but only small changes were observed here. In addition, the germanium oxidation, internal stress or even the local compositional change could effect on the peak positions (and widths as well), but is not easy at all to find out the real reason. Because of that the peak positions were not analyzed in this work [33, 34].

Table 2 and 3 show the CS/ES, CS/SE and ES/SE area ratios for different parts of the $Ge_{24}Se_{76}$ and $Ge_{28}Se_{72}$ samples with recorded gratings. Comparison of the peak area ratios shows that there are lower ES/SE and CS/SE ratios (more homopolar Se-Se bonds) and corner-sharing structural units in the $Ge_{24}Se_{76}$ film than in the $Ge_{28}Se_{72}$ layer, which is due to the higher selenium concentration of the former sample.

Blue shift of the optical absorption edge was established due to annealing below the glass transition temperature for all samples (Figure 2). In general, the annealing facilitates relaxation of the structure and brings the films closer to their equilibrium state. This was supported by the changes in Raman bands' parameters after annealing for both $Ge_{24}Se_{76}$ and $Ge_{28}Se_{72}$ samples: a more than 10% increase of CS/SE and ES/SE ratios (indicating homopolar-heteropolar bond transformation), and a slightly less remarkable of the CS/ES ratio (formation of corner-sharing units, which is in good agreement with higher amount of heteropolar bonds). This behaviour is in a good agreement with structural relaxation study on Ge-Se during annealing below T_g [35], showing that below glass softening temperature ES units transform into CS ones, which accompanies the stabilization and relaxation of the structure. So results on the annealed samples indicate that the differences in the modulation depth of the created holographic gratings (Table 1) could be related to the bonding differences and relaxation state of the structure.

The grating formation is accompanied with similar structural changes in both samples and independently on the heat treatment. It can be seen that during light induced surface patterning the CS/SE and ES/SE ratios are higher in the grating structure compared to the non-irradiated regions, with higher values for the hillocks. So, the homopolar Se-Se bonds brake up and heteropolar Ge-Se bonds (CS and ES) form due to surface patterning, which is in good agreement with observations presented in [3]. During surface patterning, lone Se atoms appear in the structure, and these presumably incorporate into the structure by forming heteropolar bonds. This mechanism is more emphasized in the hillocks suggesting that these regions are the illuminated ones, with higher level of structural changes. In addition, the simultaneous decrease of the SE area compared to both the CS and ES could be a sign of the depolymerization of the structure: some previously connected Se atoms become engaged in the fractioned tetrahedral CS and ES units. At the same time the CS/ES ratio decreases, showing that CS structural units are rearranged into ES building blocks in both $Ge_{24}Se_{76}$ and $Ge_{28}Se_{72}$ samples. The highest peak area differences were observed for the as deposited $Ge_{24}Se_{76}$ sample, and the lowest for the annealed samples.

So, the general trend of the grating formation for both compositions is the higher heteropolar bond content (higher CS/SE and ES/SE ratios) and transformation of corner-sharing structural units into edge-sharing ones.

Several papers deal with photo-induced optical, structural and volume changes in amorphous chalcogenides using near band gap light. Photoexcitation could lead to chemical bond breaking, polymerization, stress relaxation and related structural changes [12]. These structural changes could be the origin of formation of surface patterns [13, 20]. Several studies were performed to produce gratings in different ways. However, all of them interpreted the formation of surface patterns with photo-induced volume changes of the layer due to the localized structural rearrangement and ordering of Se-Se chains in selenium containing systems [7, 36-38].

We suggest that the lone Se atoms play important role in light induced surface patterning. On the microscopic level holographic grating creation could be connected with electron-hole pair excitation, defect creation, bond breaking and rearrangement in the illuminated strips. These processes are mainly related to and induced by the Se atoms, the bonds of which are sensitive to appropriate light illumination and appear as lateral mass migration in the illuminated strips, on the macroscopic level, controlled by volume diffusion as it was shown for As-Se system [36-38]. The mass transport could be connected with the gradient force of the electric field induced by light interference [39]. Non-radiative relaxations of the photoexcited carriers help this process by creating additional molecular units (oppositely charged chalcogen pairs, defects) with enhanced polarizability and by softening the matrix of the chalcogenides via bond breaking [12,27].

The importance of Se atoms in holographic grating formation is clearly indicated by the compositional dependence of the efficiency of the process, manifesting in a remarkably decreasing reaction of the material to light illumination with increasing Ge content [40]. The results obtained clearly indicate that the modulation depth of the created holographic gratings under light irradiation in Ge-Se thin films decreases with addition of Ge. Besides the composition, the observed rate of photo-induced volume changes could be connected with the structural properties of the investigated samples. There should be a connection between the structure and its photo-induced transformations, so the rigidity of the glass network of Ge-Se system influences on the investigated optical recording processes, based on the directed mass transport effects. Photons stimulate excited electron-hole pairs, non-equilibrium defects and cause mass migration under the conditions of decreased viscosity (photo-plasticity) [39]. The flexibility of the glass network depends on the composition [34].

Based on the elastic response of chalcogenides, their structural connectivity and rigidity reveals floppy, intermediate and stress-rigid phases [28]. It means that with increasing Ge content the glasses of the Ge-Se system transit from being flexible (floppy) to over-coordinated, stress-rigid. In floppy state glass network gives the possibility of large-scale response by the glass backbone under photo exposure [40]. It causes giant volume changes when such amorphous chalcogenide layers are illuminated by light. In contrast to floppy state, after floppy-rigid transformation (the crosslinking of the covalent network increases) the glass transforms to an over-coordinated rigid solid with locally stressed regions. Photons could induce relaxation in these regions, which hinders large atomic movements and influences minimal photo-induced volume changes. Network of Ge-Se samples is built with different structural fragments (ES, CS and SE) including Se chains. So, for these system the mechanism of photo-induced mass transport could be associated with elementary migration of atoms within Se chains. These acts of diffusion take place in different parts of the irradiated film and have a cooperative nature. They initiate similar processes in the neighboring structural units due to the inter-chain interactions and that leads to the volume diffusion.

The difference between the recording rate and the height of the grating in the as-deposited and annealed samples could be related to the level of uniformity (or ordering) of their structure. Layers with higher uniformity will have less spatial variation in composition, distribution of structural unit and density etc. so photo-induced changes and especially mass flow will take place smoother and faster. This supposition correlates with the data on the composition dependence on structural rigidity in this system [41, 42].

Our results show that photo-induced volume changes and the possibility of direct surface relief recording due to the mass transport in Ge-Se system under the gradient intensity of illumination demonstrate the potential of these materials for fabrication of photonic elements, as it was investigated and presented for As-Se and As-S layer structures [6-8,13,36-39,43,44].

Conclusion

The effect of deposition method and composition on the photo-induced changes was investigated in Ge-Se chalcogenide thin films, prepared by pulsed laser deposition and thermal evaporation techniques. The PLD method resulted better preservation of the composition in comparison with TE method.

The influence of heat treatment was studied as well; it results in relaxation and more uniform local structure of the layers. Detailed investigation of holographic gratings recorded in these samples by light illumination showed that efficient direct surface relief recording can be done in Ge-Se samples, especially with higher Se content. It was established that the extent of photo-induced local surface deformations, i.e. modulation

depth of the created surface structures at the same expositions decreases with increasing Ge content in Ge-Se amorphous chalcogenide layers. Giant surface patterns were obtained for Se-enriched films. Depicted photo-induced changes are caused by a lateral mass transport induced by light interference. The driving force of the mass transport is the lateral steady-state electric field. The structure and the composition play an important role in photo-induced surface patterning.

The local structure of the created surface patterns was also analyzed. Heteropolar bonds and edge-sharing tetrahedra were found to be more dominant on the hillocks, than in the valleys, suggesting the hillocks to be formed at the illuminated regions of the sample. Annealing was found to promote the grating formation through its ordering effect. Our results suggest that the lone Se atoms appearing in the structure during CS->ES transformation play a key role in photo-structural changes, mass transport and grating formation in Ge-Se chalcogenides.

Acknowledgements

Authors would like to thank to Prof. Maria Mitkova and Mr. Tyler Nichol for the enthusiastic discussion and for the valuable comments, which helped to improve the manuscript.

This work has been supported by the European Union and the State of Hungary under Grant # TÁMOP-4.2.2.A-11/1/KONV-2012-0036, which is co-financed by the European Union and the European Social Fund.

Financial support from the Czech Science Foundation (Project No. 15-02634S) is greatly acknowledged.

S. Kokenyesi and I. Csarnovics thank the IMI for New Functionality of Glass NSF, DMR 0844014 for the financial support for their research exchange visit to Boise State University, USA.

M. Veres was supported by the János Bolyai Research Scholarship of the Hungarian Academy of Sciences.

This work was supported by Defense Threat Reduction Agency under grant no: HDTRA1-11-1-0055.

References

[1]. M. Popescu, Non-Crystalline Chalcogenides, Solid State Science Technology Library, **8**, Kluwer Academic Publishers,2000.
[2]. E. Venger, A. Melnichuk, A. Stronskyi, Photostimulated processes in vitreous chalcogenide semiconductors and their applications, Academperiodica, Kiev, 2007 (in Russian).
[3]. K. Tanaka, K. Shimakawa, Amorphous chalcogenide semiconductors and related materials, Springer, New York, 2011.
[4]. H. Hisakuni, K. Tanaka, Science 270 (1995) 974.
[5]. S. N. Yannopoulos, M. L. Trunov, Phys. Stat. Solidi B 246 (2009) 1773.
[6]. Y. Kaganovskii, D. L. Beke, S. Charnovych, S. Kökényesi, M. L .Trunov, J. Appl. Phys. 110 (2011) 063502.
[7]. M. L. Trunov, P. M. Lytvyn, S. N. Yannopoulos, I. A. Szabo, S. Kökényesi, Appl. Phys. Lett. 99 (2011) 051906.
[8]. M. L. Trunov, P. M. Nagy, V. Takats, P. M. Lytvyn, S. Kokenyesi, E. Kalman, J. Non-Cryst. Solids 355 (2009) 1993.
[9]. V. I. Mikla, Yu. M. Vysochanskii, A. A. Kikineshi, D. G. Semak, Y. O. Stefanovich, Soviet Physics Journal 26 (1983) 1029.
[10]. S. Kugler, J. Hegedus, R. Lukach, J. Optoel. Adv. Mat. 9 (2007) 37.
[11]. J. Singh, Optical Properties of Condensed Matter and Applications, John Wiley & Sons, 2006.
[12]. A. Saliminia, T. V. Galstian, A. Villeneuve, Phys. Rev. Lett. **85** (2000) 41112.
[13]. J. Teteris, U. Gertners, M. Reinfelde, Phys. Stat. Solidi C 8 (2011) 2780.

[14]. V. Lyubin, M. Klebanov, A. Bruner, N. Shitrit, B. Sfez, Opt. Mater. 33 (2011) 949.
[15]. A. R. Barik, R. Naik, K. V. Adarsh, J. Non.-Cryst. Solids 377 (2013) 179.
[16]. V. Boev, M. Mitkova, P. Markovsky, P. Nagels, K. Zlatanova, Vacuum 47 (1996) 1213.
[17]. A. Singh, L. Song, R. A. Lessard, Adv. Optics 26 (1987) 2474.
[18]. J.F. Carlin, C. Zellweger, J. Dorsaz, S. Nicolay, G. Christmann, E. Feltin, R. Butte, N. Grandjean, Phys. Stat. Solidi B. 242 (2005) 2326.
[19]. V.Nazabal, F. Charpentier, J.-L. Adam, P. Nemec, H. Lhermite, M.-L. Brandily-Anne, J. Charrier, J.-P. Guin, A. Moréac, Int. J. Appl. Ceram. Technol. 8 (2011) 990.
[20]. V. Palyok, A. Mishak, I. Szabo, D. L. Beke, A. Kikineshi, Appl. Phys. A 68 (1999) 489.
[21]. E. Vateva, in Physics and Applications of Non-Crystalline Semiconductors in Optoelectronics, NATO ASI Series, Edited A. Andriesh and M. Bertolotti, Kluwer Academic Publishers, London, 1997, p. 61.
[22]. E. Vateva, G. Tschaushev, J. Optoel. Adv. Mat. 1 (1999) 9.
[23]. P. Nemec, V. Takats, A. Csik, S. Kokenyesi, J. Non-Cryst. Solids 354 (2008) 5421.
[24]. P. Nemec, S. Zhang, V. Nazabal, K. Fedus, G. Boudebs, A. Moreac, M. Cathelinaud, X.-H. Zhang, Opt. Express 18 (2010) 22944.
[25]. P. Nemec, V. Nazabal, J. Vavra, J.P. Guin, D. Vesely, A. Kalendova, M. Allix, S. Zhang, C. Drasar, Thin Solid Films, 519 (2010) 1341.
[26]. U. Gertners, J. Teteris, Optical Mat. 32 (2010) 807.
[27]. M. S. El-Bana, R. Bohdan, S. S. Fouad, J. Alloys and Compounds, 686 (2016) 115.
[28]. K. Jackson, A. Briley, S. Grossman, D. V. Porezag, M. R. Pederson, Phys. Rev. B 60 (1999) 14985.
[29]. M. T. Shatnawi, C. L. Farrow, P. Chen, P. Boolchand, A. Sartbaeva, M. Thorpe, S. J. L. Billinge, Phys. Rev. B 77 (2008) 094134.
[30]. P. Němec, J. Jedelský, M. Frumar, M. Štábl, Z. Černošek, M. Vlček, Philosophical Magazine, 84 (2004) 877.
[31]. M. Olivier, J.C. Tchahame, P. Němec, M. Chauvet, V. Besse, C. Cassagne, G. Boudebs, G. Renversez, R. Boidin, E. Baudet, V. Nazabal, Optical Material Express, 4 (2014) 525.
[32]. R. Holomb, V. Mitsa, E. Akalin, S. Akyuz, M. Sichka, J. Non-Cryst. Solids 373–374 (2013) 51.
[33]. G. Gouadec, P. Colomban, Raman Spectroscopy of Nanomaterials: How Spectra Relate to Disorder, Particle Size and Mechanical Properties, Progress in Crystal Growth and Characterization of Materials, Elsevier, 53, 2007, 1-56.
[34]. M. Micoulaut, L. Cormier, G. S. Henderson, J. Phys: Condensed Matter. 18 (2006) R753.
[35]. E. V. Aleksandrovich, V. S. Minaev, S. P. Timoshenkov, Technical Physics 60 (2015) 510.
[36]. Yu. Kaganovskii, M. L. Trunov, D. L. Beke, S. Kökényesi, Mat. Lett. 66 (2012) 159.
[37]. C. Cserháti, S. Charnovych, P. M. Lytvyn, M. L. Trunov, D. L. Beke, Yu. Kaganovskii, S. Kokenyesi, Mat. Lett. 85 (2012) 113.
[38]. M. L. Trunov, C. Cserháti, P. M. Lytvin, Yu. Kaganovskii, S. Kokenyesi, J. Phys. D.: Appl. Phys. 46 (2013) 245303.
[39]. V. Takáts, M. L. Trunov, K. Vad, J. Hakl, D. L. Beke, Yu. Kaganovskii, S. Kokenyesi, Mat. Lett. 160 (2015) 558.
[40]. L. Calvez, Z. Yang, P. Lucas, Phys. Rev. Lett. 101 (2008) 177402 (1-4).
[41]. J. Gump, I. Finkler, H. Xia, R. Sooryakumar, W. J. Bresser, P. Boolchand, Phys. Rev. Lett. 92 (2004) 245501.
[42]. P. Boolchand, K. Gunasekera, S. Bhosie, Phys. Stat. Solidi B, 1-6 (2012) / DOI 10.1002/pssb.201200368
[43]. M. L. Trunov, P. M. Lytvyn, P. M. Nagy, O. M. Dyachynska, Appl. Phys. Lett. 96 (2010) 111908.
[44]. M. Trunov, P. Lytvyn, V. Takats, I. Charnovich, S. Kokenyesi, J. Optoelectron. Adv. Mater. 11 (2009) 1959.

Table captions :

Table 1. Modulation depth of the holographic grating and induced volume change in as-deposited and annealed Ge-Se samples (h – the height of the created surface reliefs, d – the thickness of the samples)

Table 2. Area ratios of the fitted Raman bands for as-deposited (Asdep) and annealed (Ann) samples in different parts of the grating created on $Ge_{24}Se_{76}$ sample. The error of the fitting parameters was about 1 %.

Table 3. Areas ratio of the investigated Raman bands for as-deposited (Asdep) and annealed (Ann) samples in different parts of the grating created on $Ge_{28}Se_{72}$ sample. The error of the fitting parameters was about 1 %.

Figure captions:

Figure 1. Scheme of surface patterning system

Figure 2. Optical transmission spectra of as-deposited (a) and annealed (b) Ge-Se samples of different composition.

Figure 3. AFM images of the created holographic gratings on as-deposited and annealed samples: as-deposited $Ge_{24}Se_{76}$ (a), annealed $Ge_{24}Se_{76}$ (b), as-deposited $Ge_{28}Se_{72}$ (c), annealed $Ge_{28}Se_{72}$ (d).

Figure 4. Raman spectra of the as-deposited (Asdep) and annealed (Ann) samples recorded in different parts of the grating: a – $Ge_{24}Se_{76}$, b – $Ge_{28}Se_{72}$, c – Differential of the Raman spectra of the hillock and valley for annealed $Ge_{28}Se_{72}$ sample.

Table 1

Sample/Parameter	h, nm	h/d, %
$Ge_{24}Se_{76}$ As-deposited	300	60.0
$Ge_{24}Se_{76}$ Annealed	320	64.0
$Ge_{28}Se_{72}$ As-deposited	240	24.0
$Ge_{28}Se_{72}$ Annealed	480	48.0
$Ge_{30}Se_{70}$ As-deposited	22	4.4
$Ge_{30}Se_{70}$ Annealed	37	7.4
$Ge_{33}Se_{67}$ As-deposited	15	1.5
$Ge_{33}Se_{67}$ Annealed	24	2.4

Table 2

	Asdep	Hillock	Valley	Ann	AnnHillock	AnnValley
CS/SE	0.967+/-0.003	1.004+/-0.005	0.983+/-0.004	1.102+/-0.003	1.164+/-0.003	1.123+/-0.003
ES/SE	0.192+/-0.002	0.232+/-0.003	0.222+/-0.004	0.214+/-0.005	0.227+/-0.004	0.223+/-0.003
CS/ES	4.952+/-0.004	3.908+/-0.003	4.202+/-0.003	5.134+/-0.004	4.679+/-0.004	4.732+/-0.004

Table 3

	Asdep	Hillock	Valley	Ann	AnnHillock	AnnValley
CS/SE	1.562+/-0.002	1.587+/-0.007	1.572+/-0.003	1.610+/-0.002	1.682+/-0.002	1.649+/-0.007
ES/SE	0.391+/-0.002	0.412+/-.0.003	0.397+/-0.007	0.409+/-0.005	0.428+/-0.003	0.421+/-0.002
CS/ES	3.952+/-0.002	3.830+/-0.002	3.878+/-0.004	4.122+/-0.003	3.681+/-0.002	3.730+/-0.002

Figure 1

Click here to download high resolution image

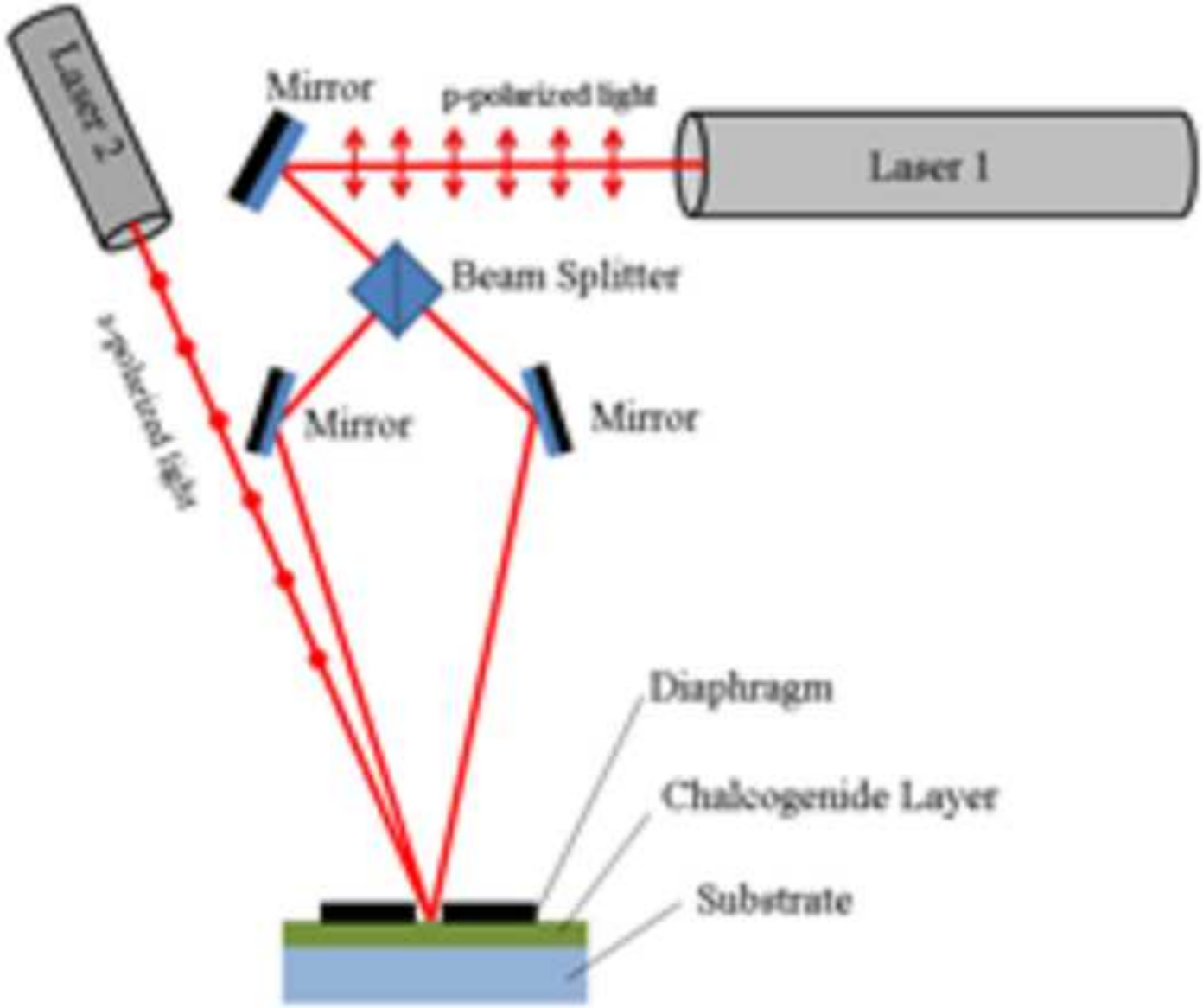

Figure 2

Click here to download high resolution image

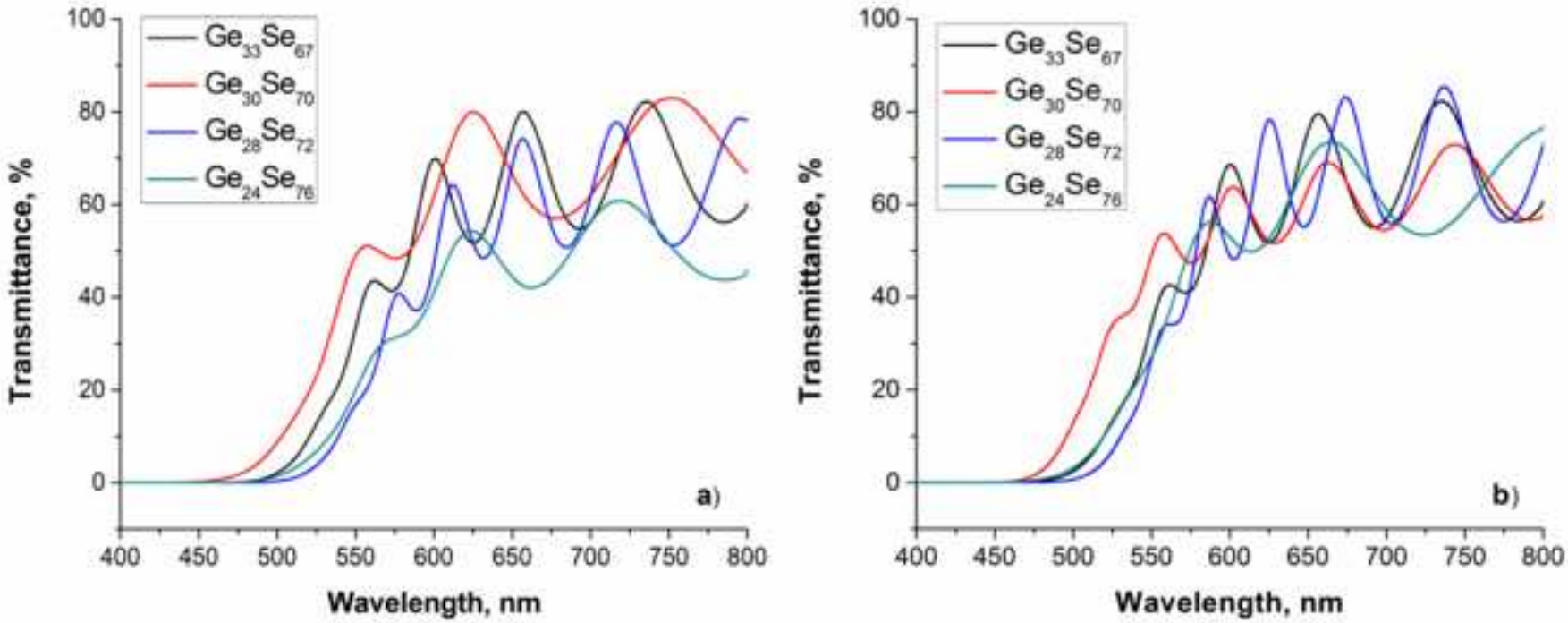

Figure 3

Click here to download high resolution image

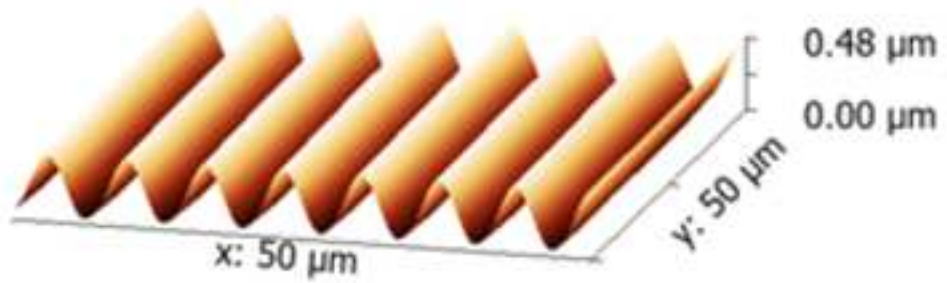

a)

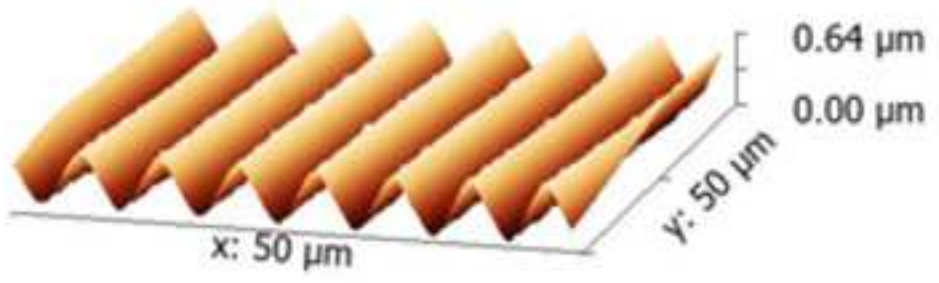

b)

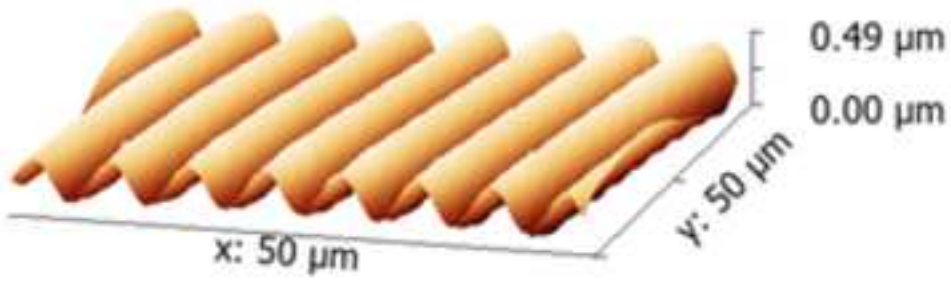

c)

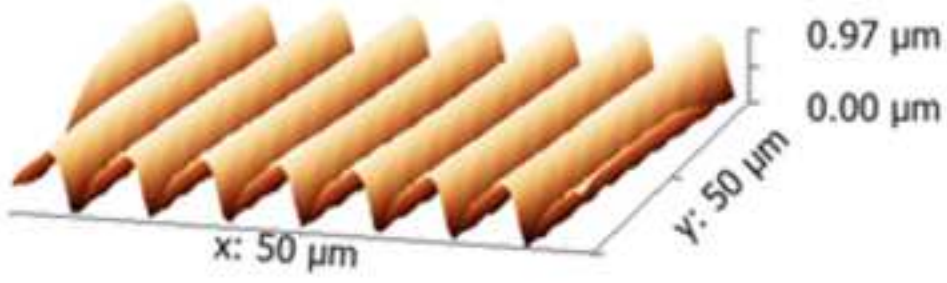

d)

Figure 4

Click here to download high resolution image